

# A LEVEL SET METHOD FOR THE MUMFORD-SHAH FUNCTIONAL AND FRACTURE

CHRISTOPHER J. LARSEN\*, CASEY L. RICHARDSON†, AND MARCUS SARKIS ‡

**Abstract.** Existing level set methods for the Mumford-Shah functional have been incapable of obtaining certain features, such as crack-tips and the presence of only triple junctions, which are known to occur in Mumford-Shah minimizers (and corresponding variational models for fracture). We introduce a new level set method for computing stationary points of certain free discontinuity problems that does obtain these critical features. Numerical experiments are presented to validate the new level set method.

**Key words.** Mumford-Shah, image segmentation, fracture, free discontinuity problem, level-set method

**AMS subject classifications.** 35, 49, 65

**1. Introduction.** The Mumford-Shah model for image segmentation ([11]) and variational models for fracture ([9]) are surprisingly similar: they both involve minimizing energies of the basic form

$$(u, \Gamma) \mapsto \int_{\Omega \setminus \Gamma} |\nabla u|^2 dx + \mathcal{H}^1(\Gamma),$$

where  $\mathcal{H}^1(\Gamma)$  is the one-dimensional Hausdorff measure (i.e., length) of the set  $\Gamma$ , representing either the boundary of images (in the case of Mumford-Shah) or the fracture set. The domain  $\Omega \subset \mathbb{R}^2$  represents either the image film or the reference configuration for the deformation  $u$ . Actually, the model for quasistatic fracture in [9] is the limit of a sequence of minimization problems of this form ([8]). For Mumford-Shah, there is the additional term

$$\int_{\Omega} |u - g|^2 dx,$$

where  $g$  is the initial image.

There has been much analysis of the properties of minimizers, mostly in the context of Mumford-Shah, and while the original Mumford-Shah conjecture – that there exists a minimizing pair in the class  $u \in H^1(\Omega \setminus \Gamma)$ ,  $\Gamma = \cup \Gamma_i$  where the union is finite and each  $\Gamma_i$  is a  $C^1$  arc – remains open (since it is still unknown whether minimizers have  $\Gamma$ 's with only a finite number of connected components), the behavior of solutions is largely understood (see [7] for a compilation of results). In particular, there is a characterization of all possible blow-up limits  $\Gamma$  of minimizing sets ([3]). The three possibilities are: i)  $\Gamma$  is a straight line (this corresponds to blowing up at a regular point of  $\Gamma$ ), ii)  $\Gamma$  is a ray, such as a crack-tip in fracture (corresponding to blowing up at such a tip), iii)  $\Gamma$  is made of three rays, meeting at a triple junction with each angle equal to  $120^\circ$ .

---

\* Department of Mathematical Sciences, Worcester Polytechnic Institute, Worcester, MA 01609 (cjlarsen@wpi.edu)

† Department of Mathematical Sciences, Worcester Polytechnic Institute, Worcester, MA 01609 (clr@wpi.edu)

‡ Instituto de Matemática Pura e Aplicada - IMPA, CEP: 22460-320, RJ, Brazil. Department of Mathematical Sciences, Worcester Polytechnic Institute, Worcester, MA 01609 (msarkis@wpi.edu).

This last property might seem odd, as it is the only junction allowed, and one might think that some minimizers would have quadruple junctions, such as in a checkerboard. However, it is not too hard to see that the total length of the boundary between the black and white squares on a checkerboard can be slightly reduced by replacing each quadruple junction with two nearby triple junctions (see figure 2.2 below), so that blow-up limits in this case are straight lines or triple junctions. We should also add that it is not known whether the type ii) “crack-tips” occur in Mumford-Shah minimizers, but this is certainly due to the fact that almost no explicit solutions are known, and the solutions that are known involve large degrees of symmetry in the domain and data. Solutions with these tips are generally believed to exist, and have been proven to exist for certain Dirichlet problems ([4]).

While  $\Gamma$ -convergence based numerical methods are theoretically justified (see, e.g., [2], [5]), there has naturally been interest in extending numerical methods for computing free boundaries to computing free discontinuities, particularly for the level set method of Osher and Sethian, [12]. Recently, Chan and Vese developed level set methods for computing the Mumford-Shah problem ([6],[14]) based on using two fields. Our interest in developing a new level set method for this problem is a result of these recent level set methods and their incompatibility with the second and third types of blow up limits, which we describe further below.

Now, we briefly outline the Vese-Chan algorithm. The starting point is the level set method for motion by mean curvature of Osher and Sethian, [12]. The idea is that, if one wants to evolve the boundary of a set  $A$  by its mean curvature, one can solve

$$\phi_t = \operatorname{div} \left( \frac{\nabla \phi}{|\nabla \phi|} \right),$$

$$\phi(0) = \text{signed distance from } \partial A.$$

Then, taking  $A(t) := \{x : \phi(x, t) < 0\}$ , it follows that  $\partial A(t)$  moves by its mean curvature. The idea for extending this to variational problems is that, if there is a necessary condition for minimality involving the mean curvature of the boundary of a set  $A$ , then an evolution law can be derived for a  $\phi$  as above, so that the set  $A(t)$  is stationary if and only if its boundary satisfies the necessary condition. Additionally, of course, one wants to design the evolution law so that if the set does not satisfy the condition, they move so that they are closer to satisfying it.

The Mumford-Shah functional is

$$\mathcal{E}(u, \Gamma) := \int_{\Omega \setminus \Gamma} (|u - g|^2 + |\nabla u|^2) dx + \mathcal{H}^1(\Gamma),$$

where  $g$  is a given  $L^\infty$  function [11]. Given  $A(0)$  and the signed distance function  $\phi$ , we consider the minimizer  $u$  of the above energy, with  $\Gamma = \partial A(0)$ . The corresponding energy can be written

$$\int_{\Omega \setminus \Gamma} E(x) dx + \mathcal{H}^1(\Gamma),$$

where  $E(x) := |u(x) - g(x)|^2 + |\nabla u(x)|^2$ . A necessary condition for minimality is that, for  $\mathcal{H}^1$  almost every  $x \in \Gamma$ ,

$$[E] = \kappa$$

for the correct orientation of the curvature  $\kappa$  (see [1]), where  $[E]$  is the jump in  $E$  across  $\Gamma$ . The idea behind this can be seen by considering the case where  $E$  is larger on one side of  $\Gamma$  than the other, and  $\Gamma$  is flat. For definiteness, we can suppose that  $\Gamma$  is horizontal and  $E$  is larger above  $\Gamma$  than below. Then it would lower the total energy to perturb  $\Gamma$  upwards into the region of larger  $E$ , and extending the solution  $u$  from below into the the region that has been newly enclosed below  $\Gamma$ . The volume term would then be reduced by  $[E]$  times the area of this region, and the surface term is increased by some amount. The equation  $[E] = \kappa$  reflects these two effects canceling each other.

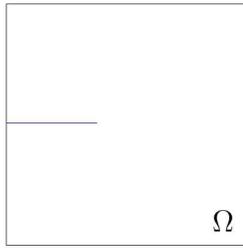
A straightforward adaptation of the level set method would then involve solving

$$\phi_t = [E] - \kappa = [E] - \operatorname{div} \left( \frac{\nabla \phi}{|\nabla \phi|} \right)$$

with appropriate initial conditions, but this would have the limitation that  $\Gamma := \partial A(0)$  can divide  $\Omega$  into only two regions: the set of points in  $A$  (i.e., where  $\phi < 0$ ) and the set of points outside (i.e., where  $\phi > 0$ ), so that, for example, triple junctions are impossible. Vese and Chan address this by using two level set functions,  $\phi^1$  and  $\phi^2$ , thereby gaining the ability to use four types of regions, or “colors”, to divide  $\Omega$ : the set where both functions are negative, the set where just  $\phi^1$  is negative, etc. However, we claim that this method retains some important deficiencies of the one-function level set method, and that the introduction of more functions does not satisfactorily overcome these deficiencies.

**2. Revisiting the Vese-Chan algorithm.** Here we identify three fundamental issues with the Vese-Chan algorithm (VCA), the first being a consequence of the inherent limitations of extending the usual level set methods to free discontinuity problems (in particular, discontinuity sets having crack-tips), the second is due to the independence of the zero level sets of the two fields in the algorithm (i.e., the fact that the two level sets do not interact with each other, for example, to combine into pairs of triple junctions when they cross, rather than forming a quadruple junction), and the third comes from the reliance on the Four Color Theorem (which would be a problem no matter how many level set functions are used).

**2.1. Crack-tips.** Since the curve  $\Gamma$  obtained by VCA is always a union of boundaries of sets, it is incapable of having a “crack tip” as illustrated in figure 2.1. Very few solutions of Mumford-Shah are known explicitly (and these tend to need very strong symmetry of the domain and data  $g$ ), and in particular there is no known solution of Mumford-Shah that has a crack-tip. However, crack-tips are known to exist in global minimizers of Mumford-Shah (see [4]), which means, essentially, that we take  $\Omega = \mathbb{R}^2$ , the  $g$  term is removed, and  $u$  is said to be minimal if it has lower energy than any  $v$  satisfying  $\{v \neq u\}$  compact support in  $\mathbb{R}^2$ , where the energy comparison is on any open set  $S$  satisfying  $\{v \neq u\}$  compact support in  $S$ . Furthermore, as mentioned above, these solutions are one of only three possible blow-up limits of solutions of Mumford-Shah. Finally, as the name “crack-tip” suggests, these solutions are of critical importance in variational models for crack growth. Indeed, Griffith’s criterion for crack growth [10], the basis for much recent work on variational methods for fracture mechanics, is a model for the growth of a crack from its tip.

FIG. 2.1. A  $\Gamma$  with a crack tip

**2.2. Triple junctions.** VCA penalizes the zero level sets of the fields  $\phi_1, \phi_2$  in a similar way to how the Mumford-Shah energy penalizes the unknown set  $\Gamma$ . The problem is that the energy contribution of the zero level sets of the two fields should be the length of the union of these sets, rather than the sum of their lengths – the difference being that when the zero level sets overlap, there is a savings. For example, without this effect, changing a quadruple junction into two triple junctions increases the energy, and so VCA will not prefer these junctions.

The fact that the lengths are penalized separately can be seen from the fact that each level set function separately satisfies the necessary condition involving curvature, independent of the fact that they might overlap. Again, this may seem insignificant, as the odds might appear to be small that these sets would overlap. However, one effect of minimizing the Mumford-Shah energy (and a source of difficulty in analyzing solutions) is that discontinuity sets prefer to overlap, so that two nearby curves can be drawn to each other in order to overlap, thereby reducing the overall energy, since each curve is effectively penalized by only half its length in the overlap region. This is not taken into account in the existing level set methods.

The fact that methods such as VCA (as well as Ambrosio-Tortorelli [2]) will generally just find local minimizers, and this phenomenon of curves moving together in order to overlap might be a property of global minimizers but not local ones, might seem to rarely affect local minimization. However, it is critical at junctions, where curves can move arbitrarily small distances to form neighboring triple junctions and decrease the energy. One result of this is that the only possible junctions are still triple junctions, since, for example, it is not hard to see from Bonnet’s characterization of global minimizers that a quadruple junction can split continuously (in  $L^2$  and  $SBV$ , etc.) into two triple junctions while decreasing the total energy (see figure 2.2). Therefore, even with local minimization, only triple junctions can occur. Yet, due to the independence of the level sets in VCA, there is no preference for these triple junctions, and any type of junction, e.g., quadruple, quintuple, can occur.

**2.3. The Four Color Theorem.** [14] relies on the Four Color Theorem in using two level set functions. The Four Color Theorem only means that a collection of objects *can* be colored using no more than four colors, and therefore two level set functions. But there must be deliberation in choosing how to color, as figure 2.3 shows: if all four colors are used in the outer four regions, there is no way to color the center region in a way that gives neighboring regions different colors. In VCA, if the initial seeding results in four “colors” for the outer objects, VCA will not detect

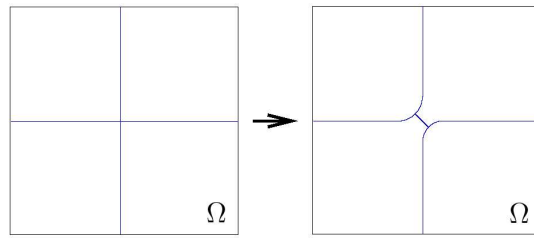


FIG. 2.2. Energy of quadruple junction can be reduced by using two triple junctions

the inner one.

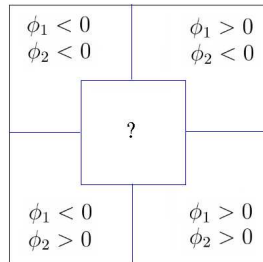


FIG. 2.3.

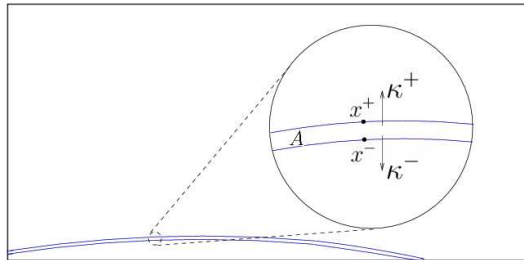


FIG. 3.1.

**3. Introduction to the proposed level set algorithm.** In seeking to develop a level set method that does not suffer from the “crack-tip” limitation, among others, it seems necessary to replace the union of curves  $\Gamma$  by a thin neighborhood  $A$  of  $\Gamma$ , and evolve this region  $A$  by a level set method. The issue is, by what law should the boundary of  $A$  evolve? Our first focus will be on a part of  $A$  approximating a curve, as in figure 3.1. If we solve for the  $u \in H^1(\Omega \setminus A)$  that minimizes

$$\int_{\Omega \setminus A} |u - g|^2 dx + \int_{\Omega \setminus A} |\nabla u|^2 dx, \tag{3.1}$$

and  $E$  is defined in the natural way so that, for the minimizer  $u$ , the above is equal to

$$\int_{\Omega \setminus A} E(x) dx,$$

then if the jump in energy from  $x^-$  “across  $A$ ” to  $x^+$ ,  $[E] := E(x^+) - E(x^-)$ , exceeds the outer curvature  $\kappa^+$  (which, for now, we assume equals  $-\kappa^-$  since  $A$  is thin), then  $\partial A$  should be perturbed upward, at both  $x^-$  and  $x^+$ . A perturbation in the opposite direction would need to follow if, instead, the curvature exceeded the energy jump.

Two problems now arise: how do we determine what point in  $\partial A$  is “across  $A$ ” from a particular  $x^- \in \partial A$ , and how do we communicate between these points to determine  $[E]$ ? We do both implicitly as follows. Notice that (assuming we have satisfactorily defined “across”) the issue is only to find the sign of

$$[E] - \kappa. \tag{3.2}$$

If we consider the quantity  $2E(x) - \kappa(x)$  at both  $x^-$  and  $x^+$ , then an easy calculation shows that (3.2) equals half of

$$(2E(x^+) - \kappa^+) - (2E(x^-) - \kappa^-).$$

Therefore, the issue is simply to determine on which side of  $A$  the quantity  $2E - \kappa$  is larger. Since  $A$  is presumed thin, a natural way to determine this, while implicitly defining “across”, is to solve

$$\Delta \psi = 0 \text{ in } A$$

$$\psi = 2E - \kappa \text{ on } \partial A.$$

Then, the normal derivative  $\partial_\nu \psi$  at any  $x^-$  indicates whether  $2E - \kappa$  is larger there, or on the other side of  $A$ . Taking  $\phi(0)$  to be the signed distance function from  $\partial A$ , negative inside  $A$ , we then solve

$$\phi_t = \partial_\nu \psi$$

for a small time step, and the updated  $A$  is then the set on which  $\phi(\Delta t) < 0$ . We again minimize (3.1) with the new  $A$ , getting an updated  $u$  and  $E$ , and resolve for  $\psi$ , etc. Of course, several issues remain, such as how to keep  $A$  thin, and these will be discussed in later sections.

The case of a crack-tip in  $\Gamma$  is somewhat different. For an  $x \in \partial A$  that is at a crack-tip, as in figure 3.2, there is no point of  $\partial A$  across from it, and so the situation is actually more straightforward and reminiscent of VCA. If  $A$  is perturbed outward at  $x$ , the region newly enclosed has zero energy, compared to  $E(x)$  before the perturbation. So, if we were penalizing the length of  $\partial A$ , we would be interested in the sign of  $E - \kappa$ , as in VCA. However, we should not penalize the length of  $\partial A$ , but rather the length of the approximated  $\Gamma$ , or 1/2 the length of  $\partial A$ . So, we are interested, again, in the sign of  $2E - \kappa$ . As  $E$  and  $\kappa$  will both be very large at a tip, and  $2E - \kappa$  will be relatively quite small away from a tip, using  $\partial_\nu \psi(x)$  to indicate the sign of  $2E - \kappa$  at a crack-tip is a reasonable approximation.

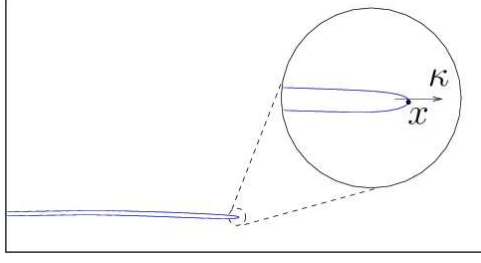


FIG. 3.2.

**4. The new level set method.** In this section we present the details of our new level set method. First, in section 4.1, we give the formal description of the new level set method. Then, in section 4.2 we give the implementation details of the algorithm.

**4.1. Formal Description.** First, given an initial image  $g$ , we seed our algorithm as follows. We find  $v \in H^1(\Omega)$  that minimizes

$$u \mapsto \int_{\Omega} |u - g|^2 dx + \int_{\Omega} |\nabla u|^2 dx. \quad (4.1)$$

We then set  $A_0$  to be the set where  $|\nabla v| \geq \gamma \|\nabla v\|_{\infty}$  for a chosen parameter  $\gamma \in (0, 1)$  and we set  $\phi(x, 0)$  to be the signed distance from  $\partial A_0$ , negative in the interior of  $A_0$  and positive outside. Then we find  $u_1 \in H^1(\Omega \setminus A_0)$  that minimizes

$$u \mapsto \int_{\Omega \setminus A_0} |u - g|^2 dx + \int_{\Omega \setminus A_0} |\nabla u|^2 dx. \quad (4.2)$$

Then we set

$$E(x) := |u_0 - g|^2(x) + |\nabla u_0|^2(x) \quad (4.3)$$

and solve the PDE

$$\begin{cases} \Delta \psi = 0 & \text{in } A_0 \\ \psi = 2E - \kappa & \text{on } \partial A_0. \end{cases} \quad (4.4)$$

Here,  $\kappa$  is shorthand for the curvature of the level sets of  $\phi$ ,

$$\kappa := \operatorname{div} \left( \frac{\nabla \phi}{|\nabla \phi|} \right). \quad (4.5)$$

Then, for any  $x \in \partial A_0$ , the sign of  $\partial_{\nu} \psi$  indicates whether  $\psi$  is larger at  $x$  or at the point  $x' \in \partial A_0$  “across” from  $x$ . For example, if

$$\partial_{\nu} \psi(x) > 0$$

then

$$\begin{aligned} 2E(x) - \kappa(x) &> 2E(x') - \kappa(x') \\ &= 2E(x') + \kappa(x), \end{aligned}$$

which reduces to

$$[E](x) := E(x) - E(x') > \kappa(x).$$

We then perturb  $A_0$  appropriately. In the context of the above example, we would perturb  $A_0$  outward at  $x$  and inward at  $x'$ . We do this by decreasing  $\phi$  at  $x$  and increasing it at  $x'$ . Thus, we solve

$$\phi_t = -\partial_\nu \psi \text{ in } \partial A_0, \quad (4.6)$$

where we note that  $\partial_\nu \phi(x') < 0$  if  $\partial_\nu \psi(x) > 0$ . This defines an approximation for  $A(\Delta t)$  given by

$$A_1 := \{x : \phi(x, \Delta t) < 0\}.$$

We then redefine  $\phi(x, \Delta t)$  to be the signed distance function from  $\partial A_1$  and we repeat this process.

**4.2. Computational details.** In this section, we present the computational details of the algorithm described above. To obtain a finite element discretization, we choose a quasi-uniform and shape-regular triangulation  $\mathcal{T}_h(\Omega)$  of  $\Omega$  composed of triangular elements of size  $O(h)$ . All computations are performed on subdomains  $\Omega' \subset \Omega$  such that no  $\partial\Omega'$  cuts through any element of  $\mathcal{T}_h(\Omega)$ , and we denote by  $\mathcal{T}_h(\Omega')$  the triangulation  $\mathcal{T}_h(\Omega)$  restricted to  $\Omega'$ . All the relevant PDEs are solved by the finite element method using the space  $V_h(\Omega') \subset H^1(\Omega')$  consisting of continuous piecewise linear functions on the triangulation  $\mathcal{T}_h(\Omega')$ .

Given a mesh  $\mathcal{T}_h(\Omega')$ , we will use the following notation for convenience:

$$\begin{aligned} \mathcal{N}(\Omega') &:= \{\text{set of all nodes } x_j \text{ in the mesh } \mathcal{T}_h(\Omega')\} \\ \mathcal{Z}_j(\Omega') &:= x_j \cup \{x_k \in \mathcal{N}(\Omega') : x_k \text{ connected to } x_j \text{ by an edge}\} \\ \mathcal{W}_j(\Omega') &:= \{\cup_k \tau_k \in \mathcal{T}_h(\Omega') : x_j \in \tau_k\}. \end{aligned}$$

We always assume that  $\tau_k$ ,  $\mathcal{W}_j$ ,  $\Omega'$  and  $\Omega$  are closed regions, and  $\mathcal{N}(\Omega')$  includes the nodes on  $\partial\Omega'$ . As part of our level set algorithm, we need to compute  $\nabla v(x_j)$  (the gradient of a function at a node  $x_j$  of  $\mathcal{N}(\Omega')$ ) for  $v \in V_h(\Omega')$ . Since  $\nabla v$  is a piecewise constant function in  $\Omega'$ , then we will need to “smooth”  $\nabla v$  to give meaning to  $\nabla v(x_j)$ . The smoothing procedure is defined via Clement interpolation, that is, using the following average of  $\nabla v$  over  $\mathcal{W}_j(\Omega')$ :

$$I_{\Omega'}^2(\nabla v)(x_j) = \frac{\sum_{\tau_k \in \mathcal{W}_j(\Omega')} \text{area}(\tau_k) \nabla v|_{\tau_k}}{\sum_{\tau_k \in \mathcal{W}_j(\Omega')} \text{area}(\tau_k)}.$$

Note that the smoothing procedure takes into account only elements  $\tau_k$  in  $\mathcal{T}_h(\Omega')$ . We also need to compute the divergence of the relevant vector fields (in particular to compute curvatures). Thus, given a vector field  $p$ , we approximate  $\nabla \cdot p$  at each  $x_j \in \mathcal{N}(\Omega')$  as follows. First, we compute a linear function defined on  $\mathcal{W}_j(\Omega')$  that is the least squares best fit of  $p_1$  evaluated at the nodes of  $\mathcal{Z}_j(\Omega')$ . We repeat this for each component of  $p$ , and then sum the slopes of the linear approximations to calculate our approximation of  $\nabla \cdot p$ .

We also use Clement interpolation to smooth the relevant scalar fields on nodes of  $\mathcal{N}(\Omega')$ . Suppose  $w$  is a scalar field defined in  $L^2(\Omega')$ . Then:

$$I_{\Omega'}^1(w)(x_j) = \frac{\sum_{\tau_k \in \mathcal{W}_j(\Omega')} \int_{\tau_k} w \, dx}{\sum_{\tau_k \in \mathcal{W}_j(\Omega')} \text{area}(\tau_k)}.$$

This smoothing procedure can be used to compute the divergence of a vector field defined on  $(V_h(\Omega'))^2$ .

We now describe the computational details of the algorithm for the first time iteration ( $n = 0$ ). Recall that we are given an image function  $g$  defined on  $\Omega$ . As described above, we begin by seeding the algorithm with a subdomain  $A_0 \subset \Omega$ . With this in mind, we minimize the problem (4.1) by the following finite element method: find  $v \in V_h(\Omega)$  such that

$$\int_{\Omega} \nabla v \cdot \nabla \varphi \, dx + \int_{\Omega} v \varphi \, dx = \int_{\Omega} g \varphi \, dx \quad \forall \varphi \in V_h(\Omega).$$

We compute  $I_{\Omega}^2 \nabla v \in V_h(\Omega)$  using the smoothing method described above, and then fix  $\gamma \in (0, 1)$  to define the subregion  $A_0 \subset \Omega$  by:

$$A_0 := \{x \in \Omega : |I_{\Omega}^2(\nabla v)(x)| \geq \gamma \max_{x_j \in \mathcal{N}(\Omega)} |I_{\Omega}^2(\nabla v)(x_j)|\}.$$

It is easy to see that  $A_0$  is a polygonal domain with edges crossing elements of  $\mathcal{T}_h(\Omega)$ . Then we define the subdomain  $A_0^h \subset A_0$  by:

$$A_0^h := \{\cup_k \tau_k \in \mathcal{T}_h(\Omega) : \text{all three vertices of } \tau_k \text{ belong to } A_0\},$$

i.e.,  $A_0^h$  is the largest subdomain of  $A_0$  composed by elements of  $\mathcal{T}_h(\Omega)$ . The definition of  $A_0^h$  and its complement  $\Omega \setminus A_0^h$  lead to natural definitions of  $\mathcal{T}_h(A_0^h)$ ,  $\mathcal{N}(A_0^h)$ ,  $V_h(A_0^h)$ ,  $\mathcal{T}_h(\Omega \setminus A_0^h)$ ,  $\mathcal{N}(\Omega \setminus A_0^h)$  and  $V_h(\Omega \setminus A_0^h)$ . These are the relevant sets for posing the finite element methods, while  $A_0$  is relevant for defining the level set function  $\phi_0$ .

We define the level set function  $\phi_0 \in V_h(\Omega)$  by computing the signed distance from each node of  $\mathcal{N}(\Omega)$  to the boundary of  $A_0$ . With the definition of  $A_0^h$  and  $\phi_0$  in hand, we solve the Dirichlet problem (4.4) by the following finite element method: find  $\psi_0 \in V_h(A_0^h)$  such that  $\psi_0(x_j) = 2E(x_j) - \kappa(x_j)$  for all nodes  $x_j$  on  $\partial A_0^h$ , and

$$\int_{A_0^h} \nabla \psi_0 \cdot \nabla \varphi \, dx = 0 \quad \forall \varphi \in V_h(A_0^h) \cap H_0^1(A_0^h). \quad (4.7)$$

To solve (4.7) we need to compute  $E(x_j)$ , defined by (4.3), and to compute the curvature  $\kappa(x_j)$ , defined by (4.5). To compute the energy  $E(x_j)$  we first find  $u_0 \in V_h(\Omega \setminus A_0^h)$  the solution of

$$\int_{\Omega \setminus A_0^h} \nabla u_0 \cdot \nabla \varphi \, dx + \int_{\Omega \setminus A_0^h} v \varphi \, dx = \int_{\Omega \setminus A_0^h} g \varphi \, dx \quad \forall \varphi \in V_h(\Omega \setminus A_0^h),$$

and then use the smoothing technique  $I_{\Omega \setminus A_0^h}^2 \nabla u_0$  described above. Similarly, we compute the curvature  $\kappa(x_j)$  by using the approximation to  $\nabla \cdot \nabla \phi_0$  as described above.

We now evolve the level set function according to (4.6). This is done by finding  $\hat{\phi}_1 \in V_h(\Omega)$  using a sort of Lax-Friedrichs discretization with a local timestepping  $\delta t_{x_j}$ :

$$\frac{\hat{\phi}_1(x_j) - I_h^1(\phi_0)(x_j)}{\delta t_{x_j}} = -\widetilde{\partial_{\nu} \psi_0}(x_j) \quad \forall x_j \in \Omega.$$

Here  $\delta t_{x_j}$  is chosen so that the zero level set curve does not move more than half of an element. The definition of the normal derivative  $\widetilde{\partial_{\nu} \psi_0} \in V_h(\Omega)$  is done as follows:

on nodes  $x_j \in \mathcal{N}(A_0^h)$ , we set  $\widetilde{\partial_\nu \psi_0}(x_j)$  to be equal to  $I_{A_0^h}^1(\nabla \psi_0 \cdot \nabla \phi_0)(x_j)$ . On the remaining nodes  $x_j \in \mathcal{N}(\Omega \setminus A_0^h) \setminus \mathcal{N}(A_0^h)$ , we take the Dirichlet data  $\widetilde{\partial_\nu \psi_0}$  on  $\partial A_0^h$  and perform the following discrete harmonic extension to  $\Omega \setminus A_0^h$ : find  $\widetilde{\partial_\nu \psi_0} \in V_h(\Omega \setminus A_0^h)$  such that

$$\int_{\Omega \setminus A_0^h} \nabla \widetilde{\partial_\nu \psi_0} \cdot \nabla \varphi \, dx = 0 \quad (4.8)$$

for all  $\varphi \in V_h(\Omega \setminus A_0^h)$  and vanishing on  $\partial A_0^h$ . The reason for using the discrete harmonic extension is because we want a smooth movement from  $\partial A_0$  to  $\partial A_1$  (the zero level set curve of  $\hat{\phi}_1$ ) when outwards from  $A_0$ . In order to decrease the complexity of the algorithm, we can replace this extension by a discrete harmonic extension to a thin layer of  $\Omega \setminus A_0^h$  near  $\partial A_0^h$ , or to replace by some local averaging away from  $\partial A_0^h$ .

Now we repeat the process. We compute the signed distance function  $\phi_1$  associated to  $\partial A_1$ , the compute  $A_1^h$ ,  $u_1$ ,  $\psi_1$ ,  $\widetilde{\partial_\nu \psi_1}$ ,  $\hat{\phi}_2$ ,  $\partial A_2, \phi_2$ ,  $A_2^h$ ,  $u_2$  etc. We point out that in regular level set methods, the level set functions  $\hat{\phi}_n$  are the ones needed for computing rather than recomputing the signed distance functions  $\phi_n$ . In our application, such a technique does not work properly because  $A_n$  is thin, and therefore, over many iterations the slope of  $\hat{\phi}_n$  might get small and new zero level sets might appear, instead of zero level sets only existing due to the evolution of the original zero level sets.

We now describe two departures from the description in 4.1 which seem to be necessary computationally. First, instead of simply solving (4.4) we actually solve the Poisson problem  $\Delta \psi = -2$ , i.e., we replace (4.7) with

$$\int_{A_0^h} \nabla \psi_0 \cdot \nabla \varphi \, dx = 2 \int_{A_0^h} \varphi \, dx \quad \forall \varphi \in V_h(A_0^h) \cap H_0^1(A_0^h). \quad (4.9)$$

This is an ad hoc technique we use to keep our domain thin. However, using this did result in our domain becoming too thin. Thus, we use another routine that enforces a minimum thickness of the domain  $A_n$ . The idea of our technique is provided in the following pseudocode:

```

for each node  $x_j$  with small  $I_h^2(\nabla \phi_n)(x_j)$ 
  if  $\text{dist}(x_j, \partial A_n) < (\text{minimum domain thickness})$ 
    set  $\frac{\hat{\phi}_{n+1}(x_j) - I_h^1(\phi_n)(x_j)}{\delta t_{x_j}} = -1$ 
  end

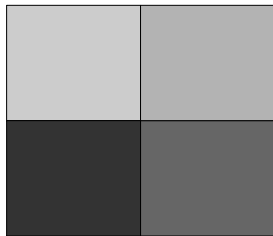
```

**5. Numerical results.** We have tested the proposed algorithm using the Mumford-Shah functional on a number of image functions, including those with overlapping objects. Also, we have verified that, when used with the energy used to model fracture, the algorithm is able to resolve crack tips.

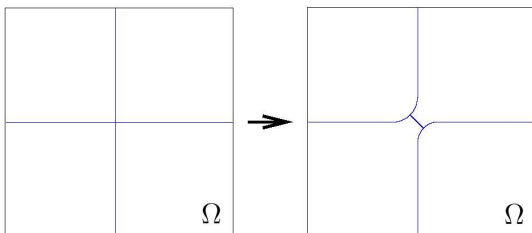
To show that our method does find triple junctions, we use the image function  $g : [0, 2] \times [0, 2] \rightarrow \mathbb{R}$  given by

$$g(x_1, x_2) := \begin{cases} 0 & \text{for } x_1 \leq 1 \text{ and } x_2 \leq 1 \\ 10 & \text{for } x_1 > 1 \text{ and } x_2 \leq 1 \\ 20 & \text{for } x_1 > \text{ and } x_2 > 1 \\ 30 & \text{for } x_1 \leq 1 \text{ and } x_2 > 1. \end{cases}$$

The corresponding image for  $g$  is pictured below in Figure 5.1.

FIG. 5.1. *Initial image function to show triple junction*

As discussed above, the minimizer of the Mumford-Shah functional for this image function does not have a quadruple junction, since the energy can be reduced by using two triple junctions:

FIG. 5.2. *Recall: Energy of quadruple junction can be reduced by using two triple junctions*

In Figure 5.3, we show the evolution of the level set curve in time obtained from our proposed new algorithm for the image function  $g$  defined above. These computations were performed on a mesh generated by Triangle [13] composed of 77,574 triangles. We applied our algorithm using an initial level set curve  $A_0$  very unrelated to the discontinuities of  $g$ . Visually we see that our algorithm captures well the discontinuities of  $g$ , and therefore, it is robust with respect to the choice of  $A_0$ . Figure 5.4 is a zoom in of the final result. We see clearly that our algorithm is effective in obtaining the triple junction. We note that the number of iterations needed to compute the solution can be reduced by seeding our algorithm with an  $A_0$  that approximates the quadruple junction created by the four color region. This approximation can be done by using the seeding algorithm described in Section 4.

**Acknowledgments.** This project began during a visit by the first author to IMPA, which also provided financial support. This material is based on work supported by the National Science Foundation under Grant No. DMS-0505660.

## REFERENCES

- [1] LUIGI AMBROSIO, NICOLA FUSCO, AND DIEGO PALLARA, *Functions of bounded variation and free discontinuity problems*, Oxford Mathematical Monographs, The Clarendon Press Oxford University Press, New York, 2000.
- [2] LUIGI AMBROSIO AND VINCENZO MARIA TORTORELLI, *On the approximation of free discontinuity problems*, Boll. Un. Mat. Ital. B (7), 6 (1992), pp. 105–123.
- [3] ALEXIS BONNET, *On the regularity of edges in image segmentation*, Ann. Inst. H. Poincaré Anal. Non Linéaire, 13 (1996), pp. 485–528.

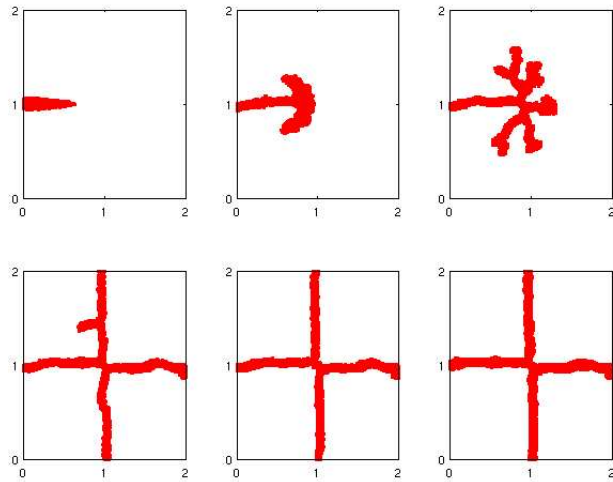
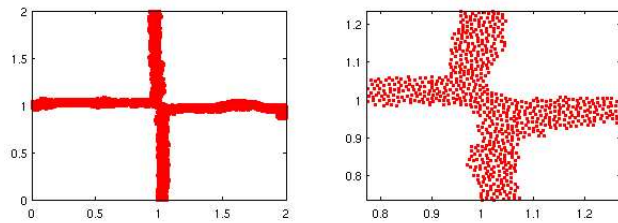
FIG. 5.3. Results of our algorithm with image  $g$ 

FIG. 5.4. Results with a zoom in on junction at right

- [4] ALEXIS BONNET AND GUY DAVID, *Cracktip is a global Mumford-Shah minimizer*, *Astérisque*, (2001), pp. vi+259.
- [5] BLAISE BOURDIN AND ANTONIN CHAMBOLLE, *Implementation of an adaptive finite-element approximation of the Mumford-Shah functional*, *Numer. Math.*, 85 (2000), pp. 609–646.
- [6] TONY F. CHAN AND LUMINITA A. VESE, *Active contours without edges*, *IEEE Transactions on Image Processing*, 10 (2001), pp. 266–277.
- [7] GUY DAVID, *Singular sets of minimizers for the Mumford-Shah functional*, vol. 233 of *Progress in Mathematics*, Birkhäuser Verlag, Basel, 2005.
- [8] GILLES A. FRANCFORT AND CHRISTOPHER J. LARSEN, *Existence and convergence for quasi-static evolution in brittle fracture*, *Comm. Pure Appl. Math.*, 56 (2003), pp. 1465–1500.
- [9] GILLES A. FRANCFORT AND JEAN-JACQUES MARIGO, *Revisiting brittle fracture as an energy minimization problem*, *J. Mech. Phys. Solids*, 46 (1998), pp. 1319–1342.
- [10] ALAN ARNOLD GRIFFITH, *The phenomenon of rupture and flow in solids*, *Phil. Trans. Roy. Soc. London*, 221-A (1920), pp. 163–198.
- [11] DAVID MUMFORD AND JAYANT SHAH, *Optimal approximations by piecewise smooth functions and associated variational problems*, *Comm. Pure Appl. Math.*, 42 (1989), pp. 577–685.
- [12] JAMES SETHIAN AND STANLEY J. OSHER, *The design of algorithms for hypersurfaces moving with curvature-dependent speed*, in *Nonlinear hyperbolic equations—theory, computation methods, and applications* (Aachen, 1988), vol. 24 of *Notes Numer. Fluid Mech.*, Vieweg, Braunschweig, 1989, pp. 544–551.
- [13] JONATHAN RICHARD SHEWCHUK, *Triangle: Engineering a 2D Quality Mesh Generator and Delaunay Triangulator*, in *Applied Computational Geometry: Towards Geometric Engineering*, Ming C. Lin and Dinesh Manocha, eds., vol. 1148 of *Lecture Notes in Computer Science*, Springer-Verlag, May 1996, pp. 203–222. From the First ACM Workshop on Applied Computational Geometry.
- [14] LUMINITA A. VESE AND TONY F. CHAN, *A multiphase level set framework for image segmen-*

*tation using the Mumford and Shah model*, International Journal of Computer Vision, 50 (2002), pp. 271–293.